Automated Region Definition for Cardiac Nitrogen-13-Ammonia PET Imaging

Otto Muzik, Rob Beanlands, Edwin Wolfe, Gary D. Hutchins and Markus Schwaiger

Division of Nuclear Medicine and Department of Internal Medicine, The University of Michigan Hospitals, Ann Arbor, Michigan

In combination with PET, the tracer ^{13}N-ammonia can be employed for the noninvasive quantification of myocardial perfusion at rest and after pharmacological stress. The purpose of this study was to develop an analysis method for the quantification of regional myocardial blood flow in the clinical setting. The algorithm includes correction for patient motion, an automated definition of multiple regions and display of absolute flows in polar map format. The effects of partial volume and blood to tissue cross-contamination were accounted for by optimizing the radial position of regions to meet fundamental assumptions of the kinetic model. In order to correct for motion artifacts, the myocardial displacement was manually determined based on edge-enhanced images. The obtained results exhibit the capability of the presented algorithm to noninvasively assess regional myocardial perfusion in the clinical environment.

J Nucl Med 1993; 34:336–344

The ability to noninvasively measure regional myocardial blood flow may significantly improve the evaluation of coronary artery disease (CAD) and its response to therapeutic interventions. The coronary reserve has been shown to provide a sensitive marker for the functional severity of coronary artery stenoses (*1*). These measurements represent functional correlates to the anatomic definition of vascular abnormalities occurring in CAD. Furthermore, accurate quantitative flow measurements in patients may enhance our understanding of various disease processes and improve subsequent treatment strategies.

Previous studies have demonstrated the capability of dynamic PET imaging methods to noninvasively measure regional myocardial perfusion (*2–5*). Recent optimization studies by Hutchins et al. (*6*) have provided a set of guidelines for definition of regions of interest (ROIs) in these methods which maximize the accuracy of the blood flow estimates. In the present study, an automated procedure for positioning ROIs on the myocardium consistent with the region of interest guidelines has been developed and tested in control subjects. In order to facilitate the implementation of this automated ROI method, it was also necessary to develop a simple motion correction algorithm to account for interstudy motion of the subject which was observed in several studies.

The specific aims of this study were to implement an automated ROI definition procedure incorporating the requirements of the tracer kinetic model; to employ a method for correction of motion artifacts in dynamic cardiac PET data; and to demonstrate the agreement between flow estimates using a traditional ROI approach with flow values derived from the automated procedure.

METHODS

Study Population

Six male volunteers (mean age 25.8 ± 3.2 yr) were studied using ^{13}N-ammonia as a blood flow agent. All subjects underwent dynamic PET imaging at baseline conditions followed by repeat imaging at pharmacologically vasodilated flow states.

Data Acquisition Protocol

Nitrogen-13-ammonia was synthesized using the method described by Gelbard et al. (*7*). Dynamic PET measurements were performed using our whole-body PET scanner Siemens 931, which allows simultaneous acquisition of 15 contiguous transaxial images with a slice thickness of 6.75 mm. The reconstructed image resolution obtained in this study was 8.5 mm ± 0.35 mm at full-width at half maximum (FWHM) in-plane and 6.6 mm ± 0.49 mm FWHM in the axial direction. A 15-min transmission scan was acquired prior to the emission study to correct for photon attenuation. After completion of the transmission scan, 15 mCi of ^{13}N-ammonia diluted in 10 cc of normal saline were administered as a slow bolus over 30 sec using a Harvard pump. At the onset of the study, a dynamic scan acquisition was initiated with varying frame duration (12 × 10 sec/4 × 15 sec/4 × 30 sec/3 × 300 sec). The total scanning time was 20 min.

After acquisition of the baseline ^{13}N-ammonia study, at least 50 min was allowed for decay of ^{13}N (physical half-life 9.9 min). During this time, residual ^{13}N activity from the preceding experiment had physically decayed to <3% of its initial activity.

Myocardial blood flow was increased by intravenous adenosine infusion of 0.14 mg/kg over 12 min. The PET data acquisition protocol was the same as described above for the baseline studies. The tracer was injected only after systolic blood pressure and heart rate were stable.

Received Apr. 22, 1992; revision accepted Sept. 2, 1992.

For correspondence and reprints contact: Markus Schwaiger, MD, Division of Nuclear Medicine, Department of Internal Medicine, University of Michigan Hospitals, 1500 E. Medical Center Drive, B1G412, Ann Arbor, MI 48109-0028.

Regional Data Analysis

Three-dimensional Reorientation. The positron emission tomograph provides 15 reconstructed transverse images oriented perpendicular to the sagittal and coronal planes of the body. Using a SUN workstation (SUN Microsystems, Inc.), 12 transaxial images were created in the short-axis view of the heart. The vertical and horizontal cardiac long-axis angles were defined using the last frame of the ^{13}N-ammonia dynamic sequence with the best tissue-to-blood ratio and were subsequently used for the reorientation of all 23 frames.

Correction for Motion Artifacts. Change in heart position of patients during the dynamic protocol can not be avoided and results in translation of the heart location. A manual correction algorithm was developed to account for motion in the x-y direction. The proposed approach relies on a clear definition of the epicardial and endocardial activity concentration edge. Because adjacent planes preserve a constant spatial position, all offset factors determined for one plane through the mid-left ventricle were applied to all remaining planes of the corresponding timepoint.

The first nine 10-sec frames of the reoriented dynamic image sequence were summed up to three 30-sec frames to improve count statistics. Offset factors determined for these combined images were later applied to each individual frame. A 3 × 3 median filter was used followed by a 3 × 3 sobel operator, resulting in a dynamic set of processed images where the epicardial and endocardial edges were sharply enhanced (Fig. 1). A reference ellipse was then adjusted in the last processed image so that it fit into these two concentric ridges. Once the size and orientation of the ellipse was defined, it was propagated to other frames in the dynamic sequence. It was then adjusted to the concentric ridges by translation, without altering the size or orientation of the ellipse (Fig. 2). Offset factors for each timepoint were determined and stored for later use.

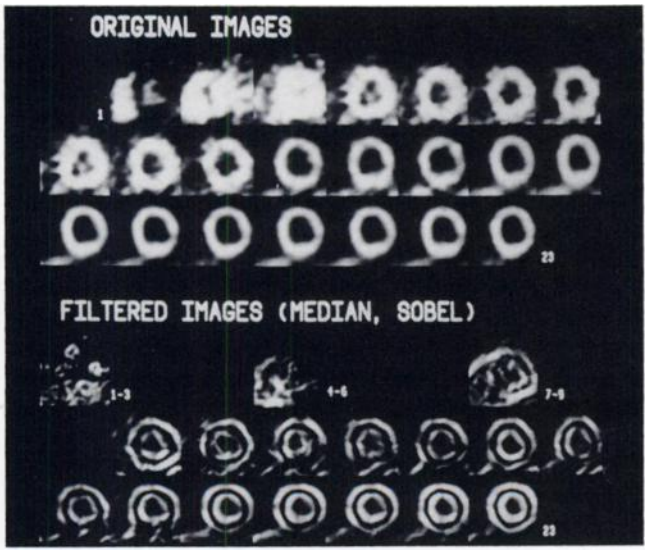

FIGURE 1. The upper part of the figure shows the original ^{13}N-ammonia activity distribution during a dynamic sequence of 23 time frames. The processed sequence after application of a median and a sobel filter is displayed in the lower part of the figure. After filtering, the epicardial and endocardial edges are sharply enhanced. Nine individual time frames are averaged to three mean images during the initial 90 sec of the processed sequence to allow acceptable recognition of myocardial edges.

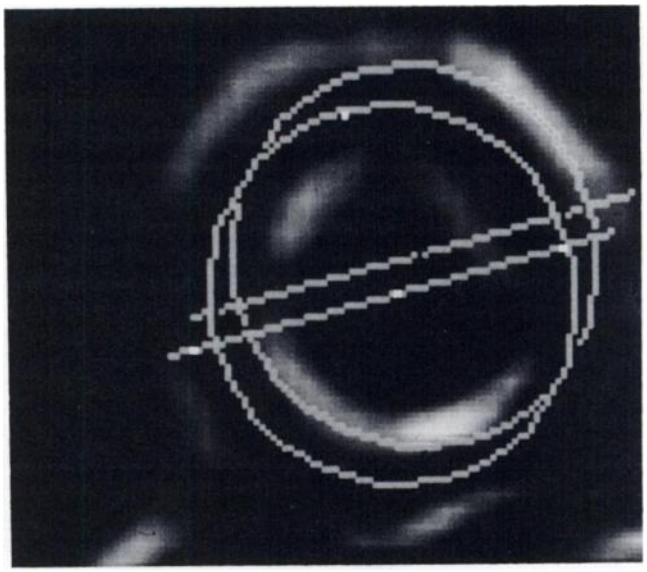

FIGURE 2. This figure shows the reference ellipse (defined at the last time frame) which is copied to an earlier time frame of the processed sequence. In the first position, the reference ellipse does not match the concentric ridge and has to be adjusted into the second position to fit into the ridge created by the myocardial edges. This translation defines the x/y offset factors for each timepoint.

Automated Definition of Myocardial and Blood Regions. The motion-corrected short-axis images served as input data to an automated regional analysis program of myocardial tracer distribution. This program involves assignment of two concentric ellipses, which enclose the myocardial activity in each of the approximately ten short-axis planes of the last time frame with the best myocardial definition. The area defined by this pair of concentric ellipses was divided into twelve 30-degree sectors representing twelve concentric myocardial regions per plane. These regions were a first rough estimate with the objective to prevent activity in the right ventricle or the liver to interfere with the automated region definition program. According to previous theoretical and experimental studies by Hutchins et al. (*6*), flow estimates with the lowest combination of bias and coefficient of variation were expected to be derived from regions characterized by a tissue-to-blood volume fraction of approximately 40:60. In order to objectively define the position matching this optimal blood volume fraction, regions were placed in relation to averaged radial profiles. Twelve averaged profiles per plane were generated from 360 individual radial profiles. Dependent on a preset threshold, a point at the inner profile flank was defined where activity reached a preset percentage of maximal activity. The circumferential borders of the regions were generated by preserving a constant distance from this threshold point in endocardial and epicardial directions (Fig. 3).

To empirically determine which combination of threshold value together with endocardial and epicardial region border distances results in the desired estimated tissue-to-blood volume fraction, image data were arbitrarily sampled in three different ways (Fig. 4). Regions I were defined at a threshold point of 75% of maximal activity along radii with three pixels in the epicardial direction and eight pixels in the endocardial direction (region width 25.8 mm). This was assumed to provide the desired tissue-

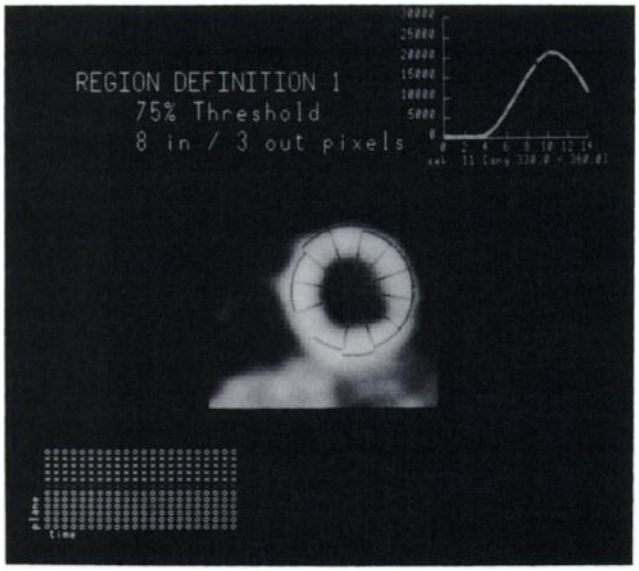

FIGURE 3. Definition of 12 myocardial sectors in the last 5-min scan of ^{13}N-ammonia activity distribution. The radial position of each sector is determined based on a mean activity profile (upper right corner). The figure shows regions defined using an inner threshold point of 75% of the maximum. From this point, the circumferential borders are defined by a distance of eight pixels to the inside and by a distance of three pixels to the outside in radial direction.

to-blood volume fraction without contamination from adjacent structures. To investigate how variations from this definition alters the blood volume fraction estimate, two other combinations were used. Regions II were defined at a threshold point of 50% of maximal activity along radii with one pixel in the epicardial direction and nine pixels in the endocardial direction (region width 23.5 mm) and Regions III were defined at a threshold point of 100% of maximal activity along radii with two pixels in the epicardial direction and four pixels in the endocardial direction (region width 14.1 mm). These regions were then propagated to other time frames.

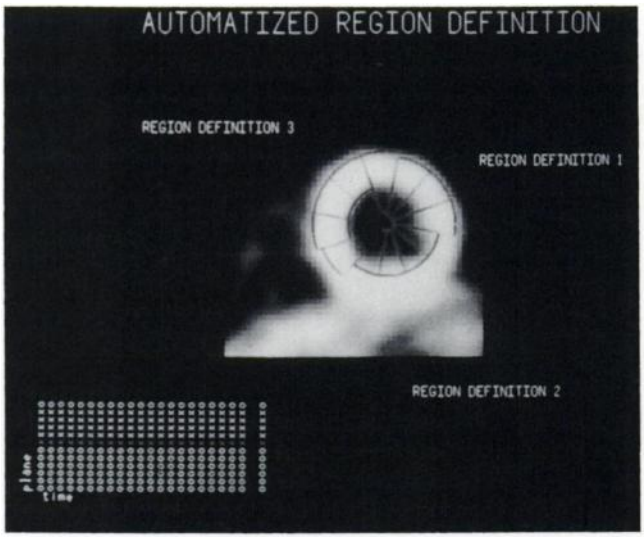

FIGURE 4. This figure displays three different sampling schemes used to test the characteristics of the automatized region definition routine. The schemes differ in the choice of the threshold point and also in the inner and outer pixel distance defining the circumferential borders.

To assess the LV blood-pool time-activity curve, a circular region was placed on the most basal plane in the resliced images. This plane was selected because it has the largest ventricular diameter allowing the placement of a large blood region in the center which was not contaminated by tissue activity spillover. The size and position of the region was adjusted by the operator based on a motion-corrected early image showing the blood peak activity in the LV pool and on the last image where myocardial tissue showed the highest tissue-to-blood ratio.

Data Analysis of Transverse Images. In order to compare the data derived using this regional analysis algorithm with data relating to myocardial blood flow published by others (*3–5*) from analysis of transverse, nonreoriented midventricular images, a second regional analysis was performed on a single transverse, midventricular image from each study. Septal, lateral and anterior regions were manually defined and extrapolated to each frame of the dynamic sequence. Before the time-activity curves were generated, the dynamic image sequence was corrected for patient motion using the same algorithm as applied to the reoriented images. The myocardial tissue regions were manually positioned in such a way that the value for the estimated blood volume fraction TBV was in the range between 50%–65%. If the fitting procedure computed a value outside this range, the region was repositioned and the fitting procedure repeated.

Myocardial Blood Flow Calculation. The model for ^{13}N-ammonia developed by Hutchins et al. (*3*) and validated (*8*) at our institution was used to calculate myocardial blood flow, which is described in detail elsewhere (*3,9*). Briefly, we have previously demonstrated that a three-compartmental model allows separation of the ^{13}N-ammonia initial extraction from retention (*3*). Based on experimental data by Schelbert et al. (*10*), the initial extraction fraction has been shown to be greater than 90%, even for flow values up to 500 ml/100 g/min. Therefore, myocardial blood flow (MBF_{NH_3}) can be expressed as:

$$MBF_{NH_3}[ml/g/min] = K_1[ml/g/min].$$

The unidirectional clearance rate K_1 is estimated by fitting the following equation to the regional time-activity curves:

$$C_m(t_i) = \frac{1}{(t_{2_i} - t_{1_i})} \cdot \int_{t_{1_i}}^{t_{2_i}} \left\{(1 - TBV)\rho_{tissue}\left[\frac{K_1 k_3}{k_2 + k_3}\int_0^T C_a(u)du + \frac{K_1 k_2}{k_2 + k_3}\int_0^T C_a(u)\cdot\exp^{-(k_2+k_3)(T-u)}du\right] + TBV\cdot C_a(T)\right\}dT, \quad \text{Eq. 1}$$

where C_m is the measured concentration by the tomograph averaged over the acquisition period and is fitted to the averaged tissue concentration predicted by the model; K_1 represents initial tracer delivery and extraction into the myocardium and carries the dimension [ml/g/min]; k_2 and k_3 are true rate constants (1/min); C_a represents the arterial blood-pool concentration; t_i is the midscan time of the i-th scan and the timepoints t_{1i} and t_{2i} mark the beginning and the end of the i-th data acquisition period; ρ_{tissue} represents myocardial tissue density [1.042 g tissue/ml tissue]; and TBV defines the total blood volume fraction (vascular and spillover contribution) in the studied region.

As described by Hutchins et al. (6), the factors (1-TBV) and TBV correct for resolution distortions caused by the finite resolution of the tomograph. Whereas contamination of tissue by blood activity is accounted for in this model, possible distortions caused by right ventricle or lung tissue spillover are not. This implies that regional sectors have to be placed in a way to match these assumptions.

Statistical Analysis

Values are given as mean ± standard deviation (s.d.). Flow values derived manually from transverse regions were correlated against flows as determined by the automated region definition procedure. Student's two-sided t-test for paired data including a Bonferonni correction for simultaneous confidence intervals was used to test the significance of the difference between: (a) flow estimates using different region definition procedures, (b) homogeneity of flow estimates determined using different region definition procedures and (c) flow estimates derived with or without motion correction. Statistical significance was defined as p values ≤ 0.05.

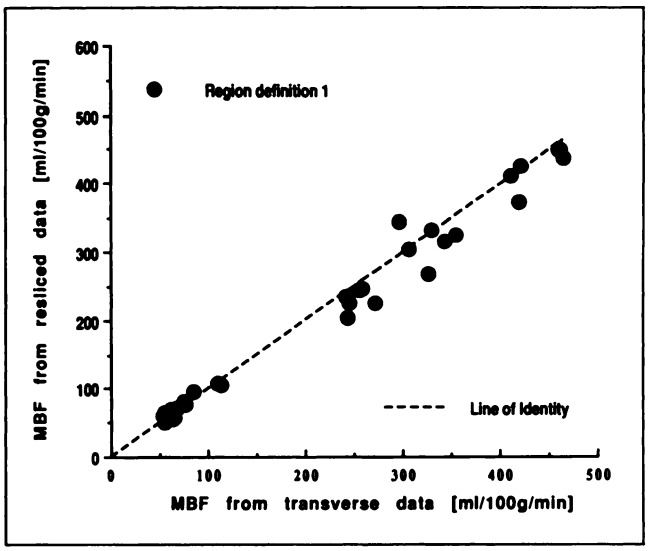

FIGURE 5. Correlation between myocardial flow estimates derived from short-axis reoriented images and flow values obtained in transverse images after motion correction was performed. Both flow estimates were highly correlated with a slope of 0.95.

RESULTS

Subjects Hemodynamics

Data from six normal subjects were analyzed with tracer injection at baseline and following pharmacological intervention. In all subjects, 12 ^{13}N-ammonia studies could be performed under stable hemodynamic conditions.

Baseline systolic and diastolic blood pressure averaged 117 ± 17/74 ± 7 mmHg and heart rate 62 ± 5 bpm. After adenosine infusion, the systolic and diastolic blood pressure values slightly decreased to 116 ± 15/70 ± 6 mmHg and heart rate increased to 82 ± 13 bpm.

Total Blood Volume Estimates

Table 1 shows rest and stress estimates of the blood volume fraction as determined by using region definitions I, II and III and as determined from transverse images. Blood volume fraction estimates were compared separately for both flow states. Blood volume fractions derived from identical procedures at rest and stress flow were statistically not significantly different. At rest and at stress flow, blood volume estimates obtained from region definition I were not significantly different from transverse blood volume estimates. According to their definition, significant differences could be found in all remaining pairwise comparisons.

Comparison of Transverse and Short-Axis Flow Estimates

Myocardial regional flow estimates derived from reoriented short-axis and transverse images agreed closely and were strongly correlated. Figure 5 shows averaged flow estimates (96 regions in 8 planes) derived from region definition I as a function of flow estimates obtained from

TABLE 1
Comparison* of Total Blood Volume (TBV) Estimates Using Different Region Definitions

Region definition	Trans	Def I	Def II	Def III	Average (n = 6) rest TBV [% blood volume] (± s.d.)
Trans	- -	-	+	+	51.5 (±7)% Trans
Def I	-	- -	+	+	54.2 (±7)% Def I
Def II	+	+	- -	+	68.3 (±6)% Def II
Def III	+	+	+	- -	34.8 (±5)% Def III
Average (n = 6)	Trans	Def I	Def II	Def III	
Stress TBV	54.0	54.7	67.7	37.2	
[% blood volume](±s.d.)	(±6)%	(±4)%	(±5)%	(±6)%	

* Paired two-sided t-test with Bonferonni correction for (n = 6) pairwise comparisons was used.

+ = significant difference in TBV ($p < 0.05$) between definition procedures detected; - = no significant difference in TBV ($p > 0.05$) detected; - - = no significant difference in TBV ($p > 0.05$) between rest and stress flow detected; Upper/lower diagonal matrix = significance levels for rest/stress TBV comparisons; Trans = large myocardial region in a transverse mid-segment plane and Def I, II, III = average over 96 regions defined using region definition I, II or III.

TABLE 2
Comparison* of Myocardial Blood Flow Estimates Using Different Region Definitions

Region Definition	Trans	Def I	Def II	Def III	Average (n = 6) rest flow [ml/100 g/min] (± s.d.)
Trans	X	-	+	-	69.0 (±17) Trans
Def I	-	X	+	-	70.3 (±18) Def I
Def II	+	+	X	+	80.2 (±22) Def II
Def III	+	+	+	X	64.6 (±17) Def III
Average (n = 6)	Trans	Def I	Def II	Def III	
Stress flow	339.5	328.9	357.8	304.6	
[ml/100 g/min](±s.d.)	(±86)	(±89)	(±100)	(±79)	

* Paired two-sided t-test with Bonferonni correction for (m = 6) pairwise comparisons was used.
+ = significant difference in flow estimates ($p < 0.05$) between definition procedures detected; - = no significant difference in flow estimates ($p > 0.05$) detected; Upper/lower diagonal matrix = significance levels for rest/stress TBV comparisons; Trans = large myocardial region in a transverse mid-segment plane and Def I, II, III = average over 96 regions defined using region definition I, II or III.

a single large region defined in a midventricular plane of the transverse image set. The best of fit line between these flow estimates was determined as $MBF_{resliced}$[ml/100g/min] = 0.948(+0.021)$MBF_{transverse}$ + 3.758(±5.233). We obtained an excellent correlation with a correlation coefficient of 0.992.

Estimates of Absolute Myocardial Blood Flow and Flow Reserve

Total myocardial blood flow was estimated separately for region definition I, II and III. Estimates were averaged over all but the most apical and most basal planes. In most studies, eight planes were included into the average. Table 2 displays average rest and stress flow values derived from transverse images and region definitions I, II and III. Furthermore, the table shows the pairwise statistical comparison between each of these values. The result of rest flow comparison demonstrates only significant differences between transverse flows and flows derived from region definition II and flows obtained using region definitions I and II, otherwise differences are not significant. At stress flow, all pairwise differences between region definition procedures differ significantly with the exception of the difference between flows derived from region definition I and transverse flows. The data indicate that an increment of blood volume fraction results in increased blood flow estimates.

Homogeneity of Flow Estimates

Regional variation of myocardial blood flow within individual studies proved to be dependent on the region definition procedure. These variations were not significantly different between baseline and vasodilated flows. The combined rest/stress coefficients of variation of flow estimates CV(FLOW) and TBV estimates CV(TBV) are displayed in Table 3. Comparison between CVs were performed separately for flow and TBV. Significant differences could be found for CF(FLOW) between region definition I and II and between region definition II and III, the difference between region definition I and III was not significant. The exact opposite relationship between region definition procedures was found for CV(TBV). Figure 6 shows the inverse relationship between CVs as determined using region definitions I, II and III. The figure indicates

TABLE 3
Comparison* Between Coefficients of Variation of Blood Flow and Between Coefficient of Variation of Total Blood Volume Estimates

Region Definition	Def I	Def II	Def III	Average† (n = 12) CV(FLOW) (± s.d.)
Def I	X	+	-	17.6 (±7)% Def I
Def II	-	X	+	35.3 (±17)% Def II
Def III	+	+	X	16.8 (±5)% Def III
Average† (n = 12)	Def I	Def II	Def III	
CV(TBV) (± s.d.)	18.3 (±7)%	14.4 (±5)%	28.3 (±13)%	

* Paired two-sided t-test with Bonferonni correction for (m = 6) pairwise comparisons was used.
† Rest and stress values combined (n = 12).
+ = significant difference in CV ($p < 0.05$) between definition procedures detected; - = no significant difference in CV ($p > 0.05$) detected; Upper diagonal matrix = significance levels for CV(FLOW) comparisons; Lower diagonal matrix = significance levels for CV(TBV) comparisons and Def I, II, III = average over 96 regions defined using region definition I, II or III.

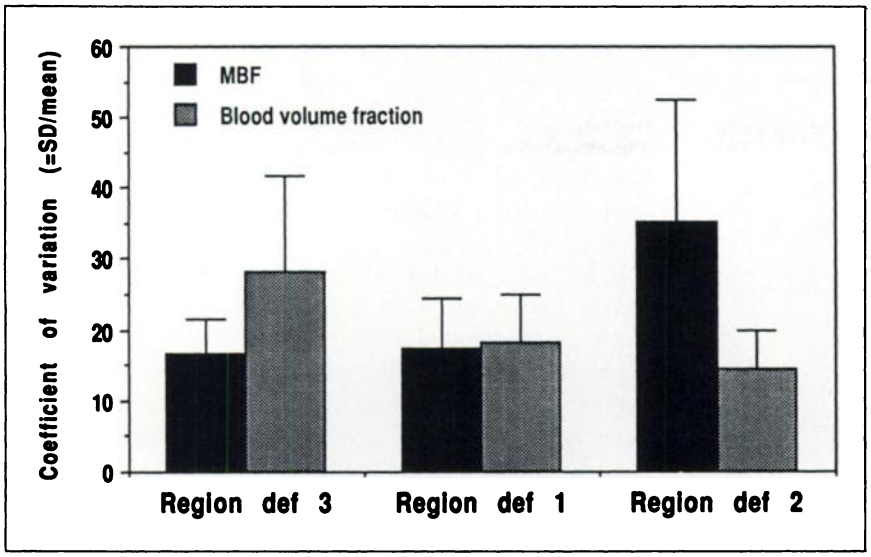

FIGURE 6. Coefficient of variation (CV = s.d.*100%/mean) for myocardial blood flow (MBF) and blood volume fraction derived from eight midventricular and basal planes averaged over all subjects studied (n = 6). The CV of flow estimates was highest for region definition II, where regions contained the highest blood volume fraction.

that regional heterogeneity of flow estimates is dependent on the blood volume fraction.

Figure 7 shows the regional flow estimates in the resting and pharmacologically vasodilated myocardium averaged over all subjects studied. Flow estimates are derived from time-activity curves obtained from region definition I (TBV = 54%), where the blood volume fraction TBV was close to the targeted blood volume fraction of 60%. The number of regions corresponding to the anatomical position was defined separately for each plane to account for the changing size of the right ventricle.

Heterogeneity of Flow Estimates Caused by Motion

To determine the variability of flow estimates caused by body motion, a paired, two-sided t-test was performed on CV(FLOW) obtained using region definition I with and without motion correction. The CV(FLOW) average decreased significantly from 22.3% ± 13.2% to 17.6% ± 6.8% after motion correction was performed ($p < 0.05$). Differences between flow estimates derived with and without motion correction were largely dependent on the individual patient study.

DISCUSSION

With use of state-of-the-art PET instrumentation and advanced image processing, absolute regional myocardial blood flow can be obtained and displayed in a polar map format. Although the concept of polar map display is widely established in SPECT cardiac imaging (*11,12*), results of nonlinear dynamic curve analysis have not been routinely displayed in this format. The results of our study show that correction for patient motion and automated region definition may be necessary to fully employ ^{13}N-ammonia as a flow tracer in clinical routine.

The reorientation of images in the short-axis view of the heart offers several advantages. It provides cross-sectional activity distributions through the heart where epicardial and endocardial edges are observed as closed circular contours. Position changes in these circular contours may

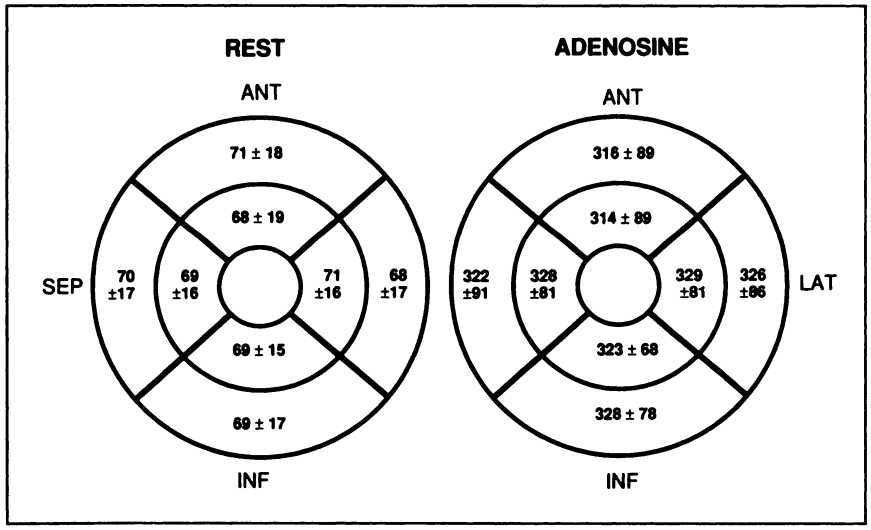

FIGURE 7. Mean regional flow estimates for the entire study population, as assessed using the region definition procedure I. In the polar representation of pooled data, the outer segments correspond to four basal planes and the inner segments to four mid-ventricular planes.

be recognized with higher accuracy than based on edge contours derived from transverse images. Furthermore, it takes full advantage of the rotational symmetry of the heart during the automated region definition procedure.

Correction for Changed Heart Position During a Dynamic Study

The presented data show that changes in heart position during the dynamic protocol affect the accuracy of flow values determined based on kinetic data analysis. In order to extract reliable kinetic parameters, procedures for image realignment are necessary for overcoming motion artifacts. In general, the correction for such misalignments consists of two steps: first, to recognize in each time frame the displacement consisting of translation, tilt and rotation (displacement parameters), and second, to realign the dynamic image sequence according to the previously determined displacement parameters.

One possible approach to determine these displacement parameters is to attach fiducial markers to the patient's body in order to monitor the movement. Although this technique has been successfully applied to brain studies (*13*), markers mounted on a patient's chest may not follow the same motion as the heart. The position of the myocardium within the chest cavity is not fixed thereby allowing torsion and displacement independent of the body surface.

Obviously, a three-dimensional approach is theoretically the most appropriate correction for patient motion. However, the mathematical problem of recognition and realignment of anatomical structures in three dimensions is not trivial (*14*), especially when considering the relatively poor myocardial definition in the early phase of the dynamic study. Furthermore, these methods are extremely demanding with respect to computation time and hardware memory requirements. Because our data are present on a slice-by-slice basis, we formulated an approximation of the exact correction procedure which is far less time consuming. No image reorientation is required as ROIs are repositioned according to the two-dimensional motion offset factors at the time of sampling.

The advantage of this method is its simplicity and its usefulness with respect to blood flow determination. It corrects for obvious misalignments between myocardial activity and ROIs which could be visually detected during the sampling procedure and caused movement artifacts in the time-activity curves. These artifacts were removed in the motion-corrected time-activity curves. The limitation of this method is due to rotation movement and motion in the third dimension (in/out plane) is not corrected. However, our results indicate that with regard to blood flow estimation, the in-plane motion seems to be the dominant distortion factor. Current development in our laboratory focuses on the development of a three-dimensional correction which can be implemented for the simple analysis of clinical ^{13}N-ammonia studies.

Automated Region Definition

Due to the finite resolution of the PET scanner, time-activity curves derived from ROIs are distorted by the partial volume effect and blood to tissue cross-contamination. Consequently, kinetic parameters derived from a compartmental model will be misrepresented when these resolution distortions are not incorporated into the modelling process.

Based on experimental work by Hutchins et al. (*6*), myocardial regions were intentionally defined in a way that they represented a combination of tissue and blood signal. The corresponding model equation (Equation 1) then combines two terms: a term representing predicted tissue concentration as a function of the rate constants and a term proportional to the blood input function. This second term accounts for both the crosscontamination of blood into tissue as well as for the vascular tissue space.

Based on dynamic information, the total blood volume fraction can be estimated from the data. According to simulation studies (*6*), the bias and variance of flow estimates derived for the ^{13}N-ammonia model approaches an optimum for a tissue-to-blood volume fraction of 40:60. Consequently, we intended to implement the automatized region definition procedure in a way to realize this optimal tissue to blood volume fraction.

The Effect of Varying Blood Volume Fractions on Flow Estimates

Region definition procedures I, II and III contained different blood volume fractions. These fractions had a significant influence on blood flow estimates; mean regional flow values increased as a function of blood volume fractions. Conversely, the homogeneity of flow estimates decreased, as the blood volume fractions increased.

ROIs defined using region definition I best realized a compromise between the requirements of the model and the clinical criterion of homogeneity. A tissue-to-blood volume fraction of 45:55 guaranteed a strong tissue signal, however, spillover from adjacent structures was negligible. The coefficient of variation of both blood flow and blood volume estimates was below 20%.

Time-activity curves derived with region definition II showed an average tissue to blood volume fraction of approximately 30:70. The high contribution of left ventricular blood pool resulted in higher flow values than obtained with region definitions I and III. Moreover, the high blood volume fraction caused an increased coefficient of variation for flow estimates and made this region definition suboptimal with regard to flow determination.

In regions defined with region definition III, the tissue-to-blood volume fraction was found to be around 65:35 with exception of the septal wall, where it was 50:50. The higher blood volume fraction in the septum was caused by activity cross-contamination from the right ventricle. Due to the relatively low temporal frequency sampling in the initial part of study, data were not sufficient to distinguish between contribution from right and left ventricular blood

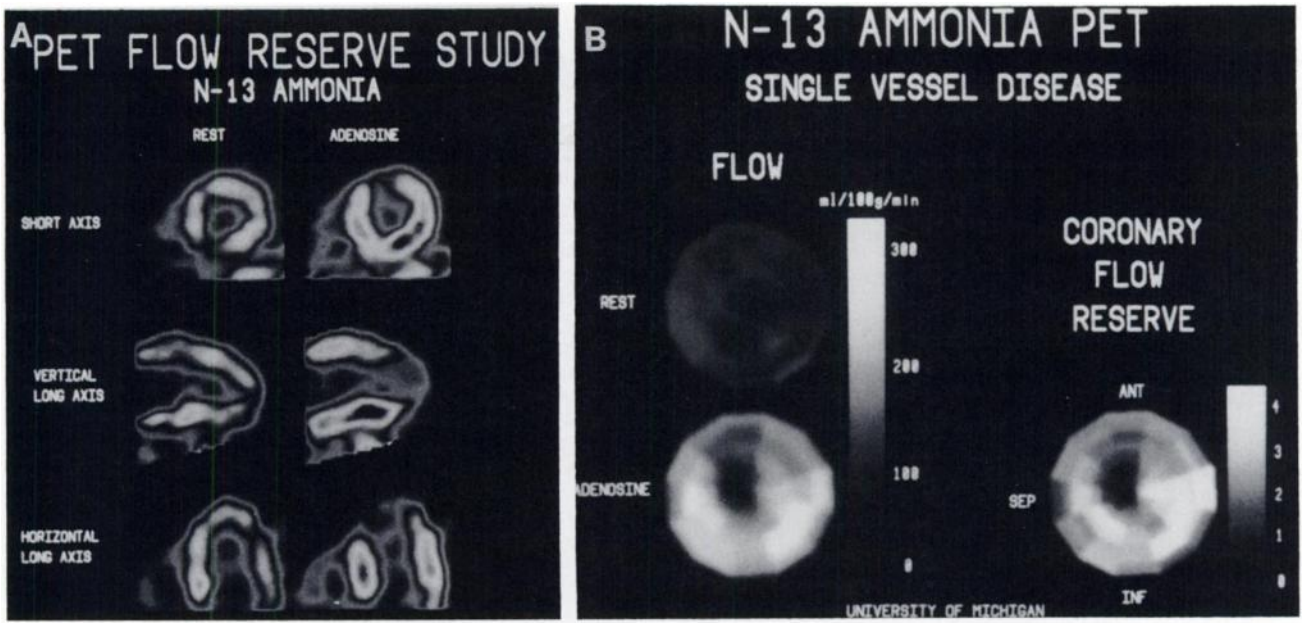

FIGURE 8. (A) Example of static ^{13}N-ammonia images of a patient suffering from coronary single-vessel disease at rest and after adenosine infusion in the short-axis, vertical long-axis and horizontal long-axis planes. Note in the postadenosine image a perfusion defect in the distal inferoseptal wall consistent with reduced retention of ^{13}N-ammonia in this region. (B) Example of a polar map display of ^{13}N-ammonia PET-derived absolute flows for the patient shown in A at rest (top left), during adenosine infusion (bottom left) and the calculated flow reserve (right). Each polar map is oriented with the base of the left ventricle at the outside and the apex in the center of the display and with the anterior wall at the top, septum on left, inferior wall at the bottom and the lateral wall on the right of the display. The flow reserve in the perfusion defect region is markedly impaired at a value of 1.7.

pool. As sectors were placed close to the epicardial edge, the low-activity spillover from lung tissue interfered with the partial volume correction and caused lower flow estimates than obtained with region definition I and II.

Problems occurred with all three region definition procedures in the apical planes where the orientation of planes was tangential to the surface of the left ventricle. The blood volume fraction in these planes could not be raised beyond 30%. The partial volume correction, which does not apply for out-of-plane partial volume effects, failed. As predicted by simulation studies, flow values in this area were underestimated by 10%–20%. In the future, orientation algorithms have to be developed which allow data sampling perpendicular to the surface of the heart throughout the whole myocardium to optimize flow estimation in the apical planes.

CONCLUSION

Dynamic PET imaging with ^{13}N-ammonia allows regional quantitative assessment of myocardial blood flow at rest and after intravenous infusion of dipyridamole; data analyzed using an automated region definition algorithm agreed well with those obtained by the widely established approach of manually derived ROIs. The study further emphasizes the importance of a correction procedure for changes in heart position. The obtained results exhibit the practicability of the ^{13}N-ammonia method for noninvasive assessment of regional myocardial perfusion in a clinical environment.

In addition to the healthy normal volunteers, we applied this technique in patients with coronary artery disease. Figure 8 shows standard static images and polar maps of one patient at rest and following adenosine infusion. The patient's polar maps demonstrate reduced maximal myocardial blood flow and flow reserve during adenosine in the perfusion defect regions corresponding to the static images. This example suggests that this method of analysis allows objective evaluation of myocardial flow and flow reserve in patients with regional flow reserve impairment. Such regional quantification of blood flow may provide accurate definition of functional significance of coronary artery disease.

ACKNOWLEDGMENTS

The authors wish to thank Steve Toorongian BS, William Walker BS and Alaa El-Deen Mourad, PhD of the Cyclotron Unit for preparation of tracer and Jill Rothley CNMT, Christine Allman CNMT, and Leslie Botti CNMT, for technical assistance obtaining the positron emission tomographic studies. They also thank Tina Bennett for skillful secretarial assistance in preparing this manuscript. This work was carried out during the tenure of an established investigatorship of Dr. Markus Schwaiger from the American Heart Association and was supported in part by the National Institutes of Health, (ROI HL41047-01) and the Department of Energy, (DOE 89-035). Dr. Otto Muzik was supported by the Austrian Erwin Schroedinger Foundation project J0473-MED. Dr. Rob Beanlands is a research fellow supported by the Heart and Stroke Foundation of Canada.

REFERENCES

1. Gould KL, Kirkeeide RL, Buchi M. Coronary flow reserve as a physiologic measure of stenosis severity. *J Am Coll Cardiol* 1990;15:459–474.
2. Iida H, Kanno I, Takahashi A. Measurement of absolute myocardial blood flow with [^{15}O]water and dynamic positron emission tomography. Strategy for quantification in relation to the partial volume effect. *Circulation* 1988; 78:104–115.
3. Hutchins GD, Schwaiger M, Rosenspire KC, Krivokapich J, Schelbert H, Kuhl DE. Non-invasive quantification of regional myocardial blood flow in the human heart using [^{13}N]ammonia and dynamic positron emission tomography imaging. *J Am Coll Cardiol* 1990;15:1032–1042.
4. Bergmann SR, Herrero P, Markham J, Weinheimer CJ, Walsh MN. Noninvasive quantification of myocardial blood flow in human subjects with [^{15}O]water and positron emission tomography. *J Am Coll Cardiol* 1989;14:639–652.
5. Krivokapich J, Smith GT, Huang SC, et al. [^{13}N] ammonia myocardial imaging at rest and with exercise in normal volunteers. Quantification of absolute myocardial perfusion with dynamic positron emission tomography. *Circulation* 1989;80:1328–1337.
6. Hutchins G, Caraher J, Raylman R. A region of interest strategy for minimizing resolution distortions in quantitative myocardial PET studies. *J Nucl Med* 1992;33:1243–50.
7. Gelbard A, Clarke L, McDonald J, et al. Enzymatic synthesis and organ distribution studies with ^{13}N-labeled L-glutamine and L-glutamic acid. *Radiology* 1975;116:127–132.
8. Muzik O, Beanlands R, Hutchins G, et al. Experimental validation of a tracer kinetic model for N-13 ammonia in comparison to O-15 water for quantification of myocardial blood flow [Abstract]. *J Nucl Med* 1991; 32:926.
9. Schwaiger M, Muzik O. Assessment of myocardial perfusion by positron emission tomography. *Am J Cardiol* 1991;67:35D–43D.
10. Schelbert H, Phelps M, Huang S, et al. N-13 ammonia as an indicator of myocardial blood flow. *Circulation* 1981;63:1259–1272.
11. Garcia E, Van Train K, Maddahi J. Quantification of rotational thallium-201 myocardial tomography. *J Nucl Med* 1985;26:17–26.
12. Hicks K, Ganti G, Mullani N, Gould K. Automated quantitation of three-dimensional cardiac positron emission tomography for routine clinical use. *J Nucl Med* 1989;30:1787–1797.
13. Evans A, Beil C, Marrett S, Thompson C, Hakim A. Anatomical-functional correlation using an adjustable MRI-based region of interest atlas with positron emission tomography. *J Cereb Blood Flow Metab* 1988;8: 513–530.
14. Faber T, Stokely E. Orientation of 3-D structures in medical images. *IEEE Trans Pattern Anal Mach Intell* 1988;10:626–633.